

Photoassociation of a Bose-Einstein Condensate near a Feshbach Resonance

M. Junker, D. Dries, C. Welford, J. Hitchcock, Y. P. Chen and R. G. Hulet

Department of Physics and Astronomy and Rice Quantum Institute, Rice University, Houston, TX 77251, USA

(Dated: November 18, 2018)

We measure the effect of a magnetic Feshbach resonance (FR) on the rate and light-induced frequency shift of a photoassociation resonance in ultracold ^7Li . The photoassociation-induced loss rate coefficient, K_p , depends strongly on magnetic field, varying by more than a factor of 10^4 for fields near the FR. At sufficiently high laser intensities, K_p for a thermal gas decreases with increasing intensity, while saturation is observed for the first time in a Bose-Einstein condensate. The frequency shift is also strongly field-dependent and exhibits an anomalous blue-shift for fields just below the FR.

PACS numbers: 03.75.Nt, 34.50.Rk, 33.80.Gj, 34.50.-s

Increasing interest in producing ultracold molecules by associating ultracold atoms has motivated an improved fundamental understanding of association processes. Photoassociation (PA) and magnetically-tuned Feshbach resonances (FR) are two ways in which gases of ultracold atoms may be connected to the molecular bound states of their underlying two-body interaction potentials. A Feshbach resonance is realized by tuning a molecular bound state near the scattering threshold [1]. The bound state perturbs the scattering state which can, in turn, strongly affect the rate of PA [2]. The rate of association of a Bose-Einstein condensate (BEC) is of particular interest, as a universal regime is predicted at extremely high rates of association [3, 4, 5, 6] where the rate is limited by a universal transient response of the atom pairs [7], independent of the underlying microscopic association process.

Several groups have measured absolute PA rate coefficients [8, 9, 10, 11, 12]. Of these, however, only two were performed with a quantum gas. In ref. [8], the rate of PA of a sodium BEC was found to increase linearly with laser intensity, without any indication of saturation. We previously investigated PA of ^7Li at the critical temperature for condensation T_c (negligibly small condensate fraction), and observed saturation at a value consistent with the maximum two-body collision rate imposed by quantum mechanical unitarity [9]. Other experiments using thermal gases have made similar observations [11, 13]. The predicted universal rate limit remains elusive. Previous experiments have also measured an intensity-dependent spectral red shift of the PA resonance [8, 9, 14], which has been ascribed to light-induced coupling to the continuum [15, 16, 17]. In this paper, measurements of the PA rate coefficient, K_p , and the spectral shift are presented in the vicinity of a magnetic FR of ^7Li for both a thermal gas and a BEC. For fields near the FR, the measured values of K_p vary by more than a factor of 10^4 . By exploiting this huge PA rate enhancement, the first evidence for saturation of the rate of PA-induced loss in a condensate is obtained. Furthermore, the FR strongly affects both the magnitude and

sign of the spectral shift.

Atomic ^7Li in the $|F=1, m_F=1\rangle$ state is prepared in a single-beam optical dipole trap, as previously described [18]. A uniform magnetic field can be set between 480–900 G to access both sides of the FR located near 736 G [19]. Evaporative cooling is achieved by reducing the optical trap beam intensity. Either Bose condensates with no discernable thermal fraction, or thermal gases with $T > T_c$, can be produced depending on the final optical trap depth.

The PA laser propagates collinearly with the optical trap beam, and is tuned to resonance (peak loss) with a vibrational level v of the $1^3\Sigma_g^+$ excited molecular state [9]. There are no unresolved rotational or hyperfine levels. For most of the measurements we tune to the $v = 83$ level, located 60 GHz below the $2^2S_{1/2} + 2^2P_{1/2}$ dissociation limit [20]. The $v = 83$ level is a good compromise between strong free-bound overlap and relatively weak off-resonance scattering from the atomic transition. Excited molecules created by the PA laser decay into pairs of energetic atoms that predominately escape the trap. The duration of the PA laser pulse τ is adjusted at each intensity I and field to maintain the fractional loss of atoms to approximately 30%. The rise and fall times of the PA pulse are less than $0.3 \mu\text{s}$. The number of remaining atoms following the laser pulse is measured using on-resonant absorption imaging.

The on-resonance loss-rate coefficient, K_p , is defined by the time evolution of the density distribution: $\dot{n}(t, \mathbf{r}) = -K_p n^2(t, \mathbf{r})$, where any possible time-dependence of K_p during the PA pulse is averaged over. For the BEC data (Fig. 4), τ is much less than either trap period, and collisional redistribution during the PA pulse can be neglected. In this case, we solve for the time-dependent density distribution analytically and extract K_p by spatially integrating the density and matching the observed and calculated loss after a time τ [8]. For much of the thermal data (Figs. 1 and 3), however, τ is comparable to the radial trap period and redistribution is not negligible. Without accounting for the details of the time evolution, we take K_p to be the average of two estimates: the first

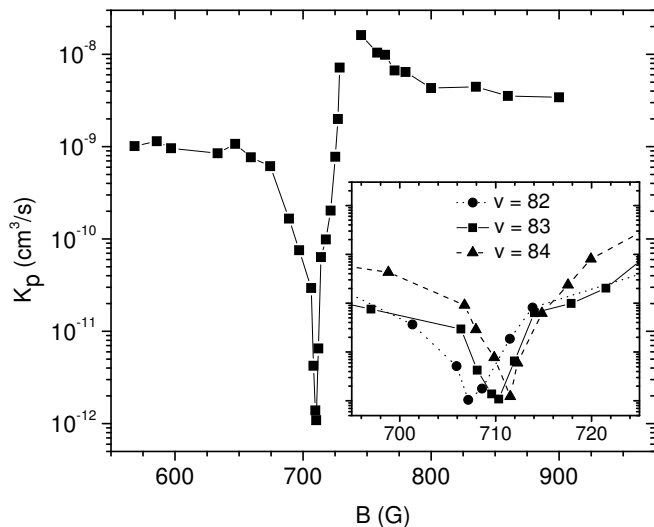


FIG. 1: K_p for PA to $v=83$ for a thermal gas. I is fixed at 1.65 W/cm^2 , while τ is adjusted between 0.07 and 270 ms to keep the fractional loss at $30 \pm 6\%$ ($\tau \propto 1/K_p$). The fitted temperatures range between $9\text{--}18 \text{ }\mu\text{K}$. The spread in initial peak density, $0.5 - 10 \times 10^{12} \text{ cm}^{-3}$, reflects a significant decrease in density near the FR, which we ascribe to enhanced three-body loss. The axial and radial trapping frequencies are 20 Hz and 3 kHz , respectively. A systematic uncertainty in K_p of 25% reflects the uncertainty in the evolution of the density (see text), as well as uncertainties in probe detuning and intensity. The statistical uncertainty is 20% . The measurement of the highest values of K_p are saturated (Fig. 3) and are therefore lower limits. The inset shows K_p (same scale as main figure) for three different excited state vibrational levels.

assumes no redistribution, as for the BEC case, while the second assumes that the distribution remains Boltzmann throughout. Due to the small fractional loss, we find the difference between the two estimates to also be small ($<25\%$), and account for it in the stated uncertainties.

Figure 1 shows the field dependence of K_p on both sides of the FR for a thermal gas. The data show a pronounced dip in K_p at 710 G , and a maximum, which is more than 10^4 times larger, located between $725\text{--}750 \text{ G}$. Measurements could not be made closer to the FR due to high inelastic collisional loss rates, presumably from a three-body process. A condensate could not be probed on the high-field side of the FR due to its instability for $a < 0$, but at a given field on the low-field side K_p for a condensate was found to be approximately half that of a thermal gas, consistent with quantum statistics.

The variation in K_p can be understood in terms of the Franck-Condon principle and the dependence of the scattering state wavefunction $f(R)$ with magnetic field (R is the internuclear separation). PA predominately occurs at the Condon radius, R_C , defined as the outer classical turning point of the excited vibrational energy state. Since $K_p \propto |f(R_C)|^2$, a node in $f(R)$ at R_C

results in a minimum in K_p . Such minima have been previously observed [21], although with much lower contrast. For sufficiently low T that the collisional wave vector k satisfies $k(R - a) \ll 1$, the asymptotic scattering state $f(R) \sim k^{1/2}(R - a)$, and a node in $f(R)$ appears at $R \simeq a$ [22]. The inset to Fig. 1 shows that the location of the K_p minima shift to higher fields (larger a) with increasing v , consistent with the fact that R_C increases with v . The peak in K_p near 736 G , on the other hand, is a manifestation of the enhancement of $f(R_C)$ when $|a|$ is large due to the FR. The ratio of the asymptotic values of K_p on the high and low field sides of the FR is ~ 3.5 , which can be understood from the ratio of $|f(R)|^2$ evaluated using the values of a at the two asymptotic fields. Using a coupled-channel calculation [23] with previously determined potentials for lithium [24], we find the scattering lengths at 600 G and 900 G to be $a_l \simeq 8 a_o$ and $a_h \simeq -43 a_o$, respectively, and $R_C \simeq 103 a_o$ for $v = 83$, where a_o is the Bohr radius. With these values, the expected ratio is $(R_C - a_h)^2 / (R_C - a_l)^2 \simeq 2.4$, in reasonable agreement with measurement.

The effect of the FR on $f(R)$ is also evident in the light-induced spectral shifts. We measured spectral shifts for both a thermal gas and a condensate for fields around the FR. The location of a PA resonance at a particular field and intensity I is determined by fitting the resonance lineshape to a Lorentzian. By taking resonance curves for several values of I , we observe that the spectral shift is linear in I , and extract the slope, Σ , plotted in Fig. 2. Far from the FR, the shift is red ($\Sigma < 0$), in agreement with previous measurements of single-photon PA [8, 9, 14]. As the FR is approached from low field, however, Σ changes sign, becoming large and positive just below the FR and large and negative just above it in a dispersive-like manner. The field where Σ vanishes (710 G), coincides with the location of the zero in K_p shown in Fig. 1.

The spectral shift is a consequence of light-induced mixing of nearby molecular states into $f(R)$, and has been shown to scale linearly with $f(R_C)$ [16]. In previous single-photon experiments the shift was dominated by coupling to the continuum, resulting in a red shift. In the case of PA near a FR, however, the shift is strongly affected by the underlying closed-channel molecular state responsible for the FR. For fields below the FR, the contribution to the shift from the bound state is positive, while above resonance it is negative.

The data of Fig. 1 demonstrate that K_p can be extraordinarily large near the FR, making it an ideal system for exploring saturation. Figure 3 shows measured values of K_p vs. I for a thermal gas at a field just above the FR. This data can be analyzed in terms of a Fano model of a bound state coupled to a continuum, where the on-resonance intensity-dependent loss rate coefficient can be

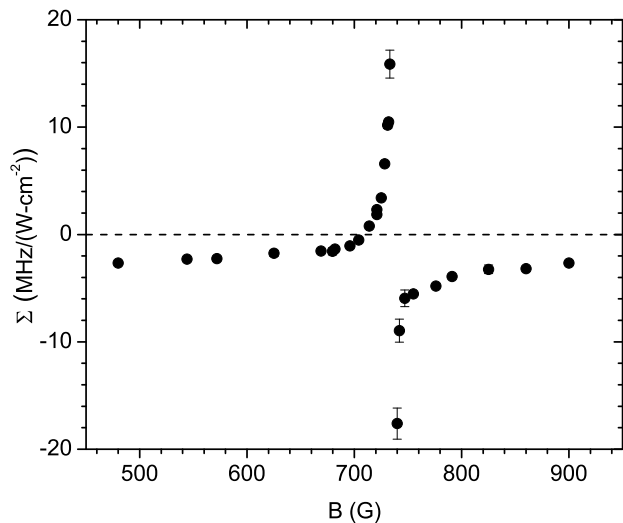


FIG. 2: Slope of the intensity-dependent spectral light shift Σ . The error bars are the standard error of the fitted slope at each field. For most of the data, this statistical uncertainty is smaller than the size of the plotted points. The systematic uncertainty in Σ is 10% due to uncertainty in I . Condensates and thermal gases were found to exhibit the same Σ .

written as [16]

$$K_p(I) = 4K_{max} \frac{I \cdot I_{sat}}{(I + I_{sat})^2}, \quad (1)$$

where K_{max} is the maximum loss rate coefficient and I_{sat} is the corresponding saturation intensity that accounts for broadening of the PA resonance. Because of the low temperatures in our experiment we neglect any energy dependence of K_p . The solid line in Fig. 3 is a fit of the data to Eq. 1. The data clearly show the predicted rollover in K_p that occurs when $I > I_{sat}$. We also observe significant power broadening that accompanies saturation. By fitting the measured lineshape to a power-broadened Lorentzian at 35 W/cm², for example, we obtain $I_{sat} = 4.3$ W/cm², in good agreement with the fit to Eq. 1, which yields 4.1 W/cm².

The theory of ref. [16] provides an estimate of the unitarity-limited maximum rate coefficient $K_u = 2k_B T \Lambda^3 / h$, where h is Planck's constant and Λ is the thermal de Broglie wavelength using the reduced mass, and the factor of 2 accounts for losing both atoms per PA event. For $T = 16$ μ K, $K_u = 8.5 \times 10^{-9}$ cm³/s, in excellent agreement with the observed maximum.

Figure 4 shows the measured intensity dependence of K_p for a BEC near the FR. By achieving extremely large FR-enhanced loss rates, saturation was observed in a condensate for the first time. The maximum K_p of 1.4×10^{-7} cm³/s is nearly a factor of 10 larger than for any previous PA rate measurement [9].

A complete theoretical understanding of PA of a BEC in the high-intensity regime is still evolving, but a frame-

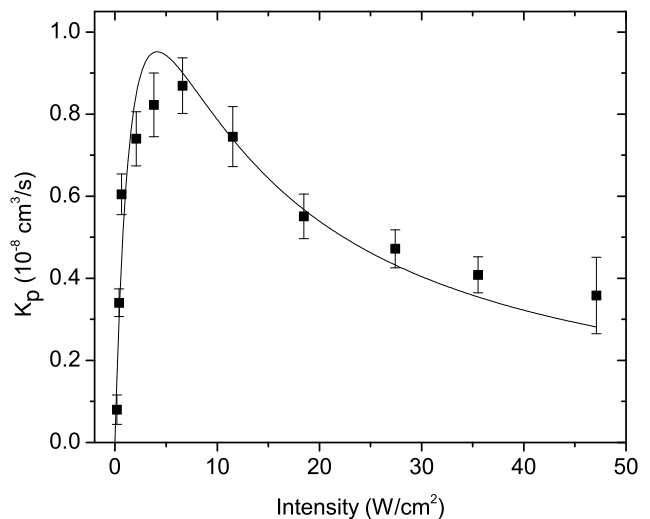


FIG. 3: K_p vs. I in a thermal gas at 755 G. $T \simeq 16$ μ K and the peak density is 7.5×10^{11} cm⁻³. τ is between 210–250 μ s for all of the data except at the lowest intensity, for which $\tau = 2$ ms. The error bars are the statistical uncertainties from the fitted T . The systematic uncertainties are 30% for K_p and 10% for I . The solid line is a weighted fit to the data using Eq. 1, with the fitted parameters $K_{max} = 9.5 \times 10^{-9}$ cm³/s and $I_{sat} = 4.1$ W/cm². A linear fit to the slope for small I gives $8.2 \pm 1.1 \times 10^{-9}$ cm³ s⁻¹/(W cm⁻²), where the uncertainty refers only to statistical uncertainty.

work for comparison of the data may be established by defining K_p in terms of a characteristic length, L , as $K_p = (\hbar/m)L$. The smallest relevant length scale is the average interatomic separation, evaluated at the peak density n_o . Taking $L = n_o^{-1/3}$, we obtain the “rogue photodissociation” limit, K_{pd} , a universal regime where saturation in the rate of condensate loss is predicted due to the dissociation of excited molecules into the hot pair continuum [3]. The NIST BEC experiment achieved $K_p \simeq K_{pd}$, but with no indication of saturation [8]. For the data of Fig. 4, $n_o = 1.6 \times 10^{12}$ cm⁻³, giving $K_{pd} \sim 8 \times 10^{-9}$ cm³/s. Our measured K_{max} is nearly 20 times greater than K_{pd} . More recent calculations [5, 7], however, have shown that while dissociation does impose a rate limit on condensate loss, it is not as stringent as K_{pd} . While the highest- I data of Fig. 4 are well into the “dissociation regime” [6, 7], our measured K_{max} is, nonetheless, nearly 7 times greater than predicted from the equations given in ref. [7]. We note that in the experiment atoms removed from the condensate but left with energies below the trap depth (500 nK) may be indistinguishable from condensate atoms by our detection method. This effect cannot explain the discrepancy with theory, however, as it would result in an apparent suppression of K_p at the onset of photodissociation.

The observed saturation could be explained by a higher than expected limit imposed by dissociation, perhaps due

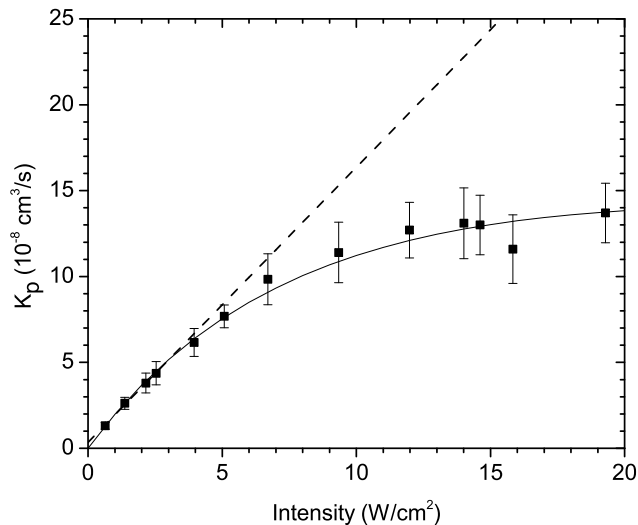


FIG. 4: K_p for a BEC at 732 G ($a \simeq 1000 a_0$). The $1/e^2$ intensity radius of the PA beam of $560 \mu\text{m}$ is much larger than the radial Thomas-Fermi radius of the BEC. The pulse duration $\tau \propto 1/K_p$, is $3 \mu\text{s}$ for the highest I and $50 \mu\text{s}$ for the lowest. The peak density is $1.6 \times 10^{12} \text{ cm}^{-3}$. The axial and radial trapping frequencies are 4.5 Hz and 200 Hz, respectively. The solid line is a fit to Eq. 1 with fit parameters $K_{max} = 1.4 \times 10^{-7} \text{ cm}^3/\text{s}$ and $I_{sat} = 26 \text{ W}/\text{cm}^2$. A linear fit to the low intensity data gives a slope of $1.6 \times 10^{-8} \text{ cm}^3 \text{ s}^{-1}/(\text{W cm}^{-2})$, as indicated by the dashed line. The error bars are the statistical uncertainties, due mainly to the measured Thomas-Fermi radius of the initial density distribution. A systematic uncertainty of 12% reflects the uncertainty in the image probe detuning and intensity. I could not be increased further without producing loss from dipole forces.

to cross-coupling between the PA and Feshbach resonances [25]. An alternative explanation is provided by quantum mechanical unitarity. If we take $L \sim 2R_{TF}$, where $R_{TF} \simeq 10 \mu\text{m}$ is the radial Thomas-Fermi radius, then $K_u \sim 1.8 \times 10^{-7} \text{ cm}^3/\text{s}$, in good agreement with the measured value of $1.4 \times 10^{-7} \text{ cm}^3/\text{s}$. A preprint has recently appeared that directly models our experiment with good quantitative results [25], but it does not determine whether the rate limit is imposed by dissociation or unitarity.

We have presented well-characterized measurements of PA near a FR, which we hope will serve to constrain and guide theory, especially in the previously unexplored strong coupling regime. Condensate loss rates as high as the unitarity limit have been demonstrated by combining PA and Feshbach resonances. Future studies should explore the dynamical behavior of loss since K_p is predicted to be time-dependent in the dissociation regime [3, 5, 6, 7]. Finally, Feshbach enhanced PA may prove useful in realizing the long-sought goal of coherent oscillation between atomic and molecular condensates [26] or for efficient production of ground-state molecules [27]

using a two-photon process [28].

We thank T. Corcovilos, R. Côté, T. Gasenzer, P. Julienne, T. Killian, M. Mackie, P. Naidon, G. Partridge, and H. Stoof for valuable discussions. Support for this work was provided by the NSF, ONR, the Keck Foundation, and the Welch Foundation (C-1133).

-
- [1] E. Tiesinga, B. J. Verhaar, and H. T. C. Stoof, Phys. Rev. A **47**, 4114 (1993).
 - [2] F. A. van Abeelen, D. J. Heinzen, and B. J. Verhaar, Phys. Rev. A **57**, R4102 (1998); Ph. Courteille *et al.*, Phys. Rev. Lett. **81**, 69 (1998); B. Laburthe Tolra *et al.*, Europhys. Lett. **64**, 171 (2003).
 - [3] J. Javanainen and M. Mackie, Phys. Rev. Lett. **88**, 090403 (2002).
 - [4] K. Góral, M. Gajda, and K. Rzążewski, Phys. Rev. Lett. **86**, 1397 (2001); M. Holland, J. Park, and R. Walser, Phys. Rev. Lett. **86**, 1915 (2001).
 - [5] T. Gasenzer, Phys. Rev. A **70**, 043618 (2004).
 - [6] P. Naidon and F. Masnou-Seeuws, Phys. Rev. A **73**, 043611 (2006).
 - [7] P. Naidon, E. Tiesinga, and P. S. Julienne, Phys. Rev. Lett. **100**, 093001 (2008).
 - [8] C. McKenzie *et al.*, Phys. Rev. Lett. **88**, 120403 (2002).
 - [9] I. D. Prodan *et al.*, Phys. Rev. Lett. **91**, 080402 (2003).
 - [10] R. Wester *et al.*, App. Phys. B **79**, 993 (2004).
 - [11] S. D. Kraft *et al.*, Phys. Rev. A **71**, 013417 (2005).
 - [12] P. G. Mickelson *et al.*, Phys. Rev. Lett. **95**, 223002 (2005).
 - [13] U. Schlöder *et al.*, Phys. Rev. A **66**, 061403(R) (2002); C. Haimberger *et al.*, J. Phys. B **39**, S957 (2006); M. Jie *et al.*, Chin. Phys. Lett. **24**, 1904 (2007).
 - [14] J. M. Gerton, B. J. Frew, and R. G. Hulet, Phys. Rev. A **64**, 053410 (2001); M. Portier *et al.*, J. Phys. B **39**, S881 (2006).
 - [15] P. O. Fedichev, M. W. Reynolds, and G. V. Shlyapnikov, Phys. Rev. Lett. **77**, 2921 (1996).
 - [16] J. L. Bohn and P. S. Julienne, Phys. Rev. A **60**, 414 (1999).
 - [17] A blue-shift was observed in the second step of two-photon PA which terminated in the ionizing continuum: K. M. Jones *et al.*, J. Phys. B **30**, 289 (1997).
 - [18] Y. P. Chen *et al.*, Phys. Rev. A **77**, 033632 (2008).
 - [19] The data of Fig. 2 place the center of the FR at 736 ± 1 G, which is a somewhat higher field than obtained in a lower resolution measurement reported previously by K. E. Strecker *et al.*, Nature **417**, 150 (2002).
 - [20] E. R. I. Abraham *et al.*, J. Chem. Phys. **103**, 7773 (1995).
 - [21] V. Vuletić *et al.*, Phys. Rev. Lett. **83**, 943 (1999).
 - [22] R. Côté *et al.*, Phys. Rev. Lett. **74**, 3581 (1995).
 - [23] M. Houbiers *et al.*, Phys. Rev. A **57**, R1497 (1998).
 - [24] E. R. I. Abraham *et al.*, Phys. Rev. A **55**, R3299 (1997).
 - [25] M. Mackie *et al.*, arXiv:0804.3011.
 - [26] D. J. Heinzen *et al.*, Phys. Rev. Lett. **84**, 5029 (2000).
 - [27] S. J. J. M. F. Kokkelmans, H. M. J. Vissers, and B. J. Verhaar, Phys. Rev. A **63**, 031601(R) (2001).
 - [28] E. R. I. Abraham *et al.*, Phys. Rev. Lett. **74**, 1315 (1995); R. Wynar *et al.*, Science **287**, 1016 (2000).